

Article

# ABCB1 does not require the side-chain hydrogen-bond donors Q347, Q725, Q990 to confer cellular resistance to the anticancer drug taxol

Keerthana Sasitharan <sup>1</sup>, Hamzah Asad Iqbal <sup>1</sup>, Foteini Bifsa <sup>1</sup>, Aleksandra Olszewska <sup>1</sup> and Kenneth J. Linton \*

Blizard Institute, Barts and the London School of Medicine and Dentistry, Queen Mary University of London, 4 Newark St, London E1 2AT

<sup>1</sup> contributed equally to this research

\* Correspondence: k.j.linton@qmul.ac.uk; Tel.: +44 (0)207 882 8997

**Abstract:** The multidrug efflux transporter ABCB1 is clinically important for drug absorption and distribution and can be a determinant of chemotherapy failure. Recent structure data shows that three glutamines donate hydrogen bonds to co-ordinate taxol in the drug binding pocket. This is consistent with earlier drug structure-activity relationships that implicated the importance of hydrogen bonds in drug recognition by ABCB1. By replacing the glutamines with alanines we have tested whether any or all of Q347, Q725 and Q990 are important for the transport of three different drug classes. Flow cytometric transport assays show that Q347A and Q990A act synergistically to reduce transport of Calcein-AM, BODIPY-verapamil and OREGON GREEN-taxol bisacetate but the magnitude of the effect was dependent on the test drug and no combination of mutations completely abrogated function. Surprisingly, Q725A mutants generally improved transport of Calcein-AM and BODIPY-verapamil, suggesting that engagement of the wild-type Q725 in a hydrogen bond is inhibitory for the transport mechanism. To test transport of unmodified taxol, stable expression of Q347/725A and the triple mutant was engineered and shown to confer equivalent resistance to the drug as the wild-type transporter, further indicating that none of these potential hydrogen bonds between transporter and transport substrate are critical for function of ABCB1. The implications of the data for plasticity of the drug binding pocket are discussed.

**Keywords:** P-glycoprotein; multidrug resistance; ABCB1; taxol; drug transport; ABC transporter

## 1. Introduction

Multidrug resistance (MDR) remains a problem for the chemotherapy of cancer patients (1, 2). Polyspecific efflux transporters of the plasma membrane that prevent the accumulation of a range of cytotoxic drugs to cytotoxic levels are a common cause of MDR (3, 4). The primary transporter associated with failure of chemotherapy is ABCB1 (previously known as P-glycoprotein and MDR1). Outside of the cancer clinic ABCB1 is an important determinant of drug absorption, distribution and excretion of many drugs including antibiotics, anti-epileptics and antiarrhythmics due to its native expression in a range of tissues including the apical membranes of gut epithelia and endothelial cells of the blood brain barrier, and the canalicular membrane of the liver hepatocytes (5). The polyspecificity of ABCB1 for many drugs of different structure and chemical class is a key feature of the transporter that needs to be understood to allow design of drugs to avoid recognition by the transporter and the design of specific inhibitors. In this regard, the recent report by Alam *et al.*, (6) of the structure of ABCB1 in complex with a transport substrate, the anticancer drug taxol, is a milestone in the field. The complex was solved by single particle imaging using cryoelectron microscopy with the taxol molecule occluded within the transmembrane domains of the transporter. Twelve amino acids were highlighted to coordinate the drug. Of these, only three glutamines, Q347, Q725 and Q990, located respectively in transmembrane helix (TMH) 6, TMH7 and TMH12, form hydrogen

bond contacts. The study is not without limitations: the medium resolution of 3.5Å, the low level of functional activity of the transporter within the nanodisc particles and the trapping of the transporter conformation using an inhibitory antibody may impact the physiological significance of the findings. The impact these have on the veracity of structural detail remain unclear and the implications of the binding pocket were not tested further. However, structure-activity studies had previously implicated the importance of hydrogen bonds in drug recognition by ABCB1 (7, 8). The simplest interpretation of these earlier structure-activity relationship data and the recent empirical structural data is that the three glutamines are likely key to drug recognition. In the current study we ask whether any or all of the glutamines are necessary for triggering the transport cycle and whether they have a role in the polyspecificity of the transporter. The glutamines were replaced with alanine residues to create single, paired and triple mutants. We measured the effect on the transport efficiency of three different classes of drug in transiently-transfected cells and test whether the mutants are able to confer resistance to taxol on stable expression in Flp-In cells.

## 2. Materials and Methods

### 2.1 Site-Directed Mutagenesis

The cDNA encoding ABCB1 including a 12 histidine carboxy-terminal tag was described previously (9). This cDNA was subcloned into pCI-neo to generate pCI-neo-ABCB1-12his (henceforth designated pABCB1). The coding sequence was modified by Lightning site-directed mutagenesis (Agilent Technologies) following the manufacturers recommendations except for generation of the Q347A mutant where a lower annealing temperature of 50°C was required. The individual mutants were made first then the second and third mutations added sequentially. Each cDNA was fully sequenced to ensure veracity.

Mutagenic oligonucleotides with the new alanine codons emboldened:

Q347A

Forward; 5'-ttaattggggcttttagtgttgga**gcgg**catctccaagcat-3'

Reverse; 5'-atgcttgagatg**ccg**ctccaacactaaaagccccaattaa-3'

Q725A

Forward; 5'-gtgccattataaatggaggcctg**gc**caccagcattgcaataatattt-3'

Reverse; 5'-aaaatattattgcaaatgctg**gtg**ccaggcctcattataatggcac-3'

Q990A

Forward; 5'-gccatggccgtgggg**gc**agtcagttcatttgc-3'

Reverse; 5'-gcaaatgaactgact**g**ccccacggccatggc-3'

### 2.2 Transient Expression of ABCB1

HEK293T cells were grown in DMEM high glucose (ThermoFisher Sci) supplemented with 10% foetal bovine serum (FBS; ThermoFisher Sci) at 37°C in a humidified incubator with 5% CO<sub>2</sub>. For transient transfection 1.2 x10<sup>6</sup> cells were seeded onto a T25 culture flask. Twenty four hours post seeding the cells were transfected with 10 µg plasmid DNA in complex with 15 µg linear polyethylenimine (Sigma Aldrich). Cells were cultured for a further 48 hrs before harvesting with TrypLE (ThermoFisher Sci) and quenching of the trypsin with culture medium.

### 2.3 Drug transport assay

Transiently-transfected HEK293T cells (5 x 10<sup>5</sup>) were incubated at 4°C for 20 min with 0.5 µg anti-ABCB1 antibody (4E3; Abcam) in transport buffer (DMEM, high glucose (4.5g/L), minus phenol red, supplemented with 1% FBS. The cells were pelleted at 500 G for 2 min and the supernatant discarded. The cells were washed once in transport buffer and resuspended in warm (37°C) transport buffer containing 2.5 µg goat anti-mouse secondary conjugated to recombinant phycoerythrin (RPE; Dako) and one of three green-

fluorescent drugs at a final concentration, unless otherwise stated, of 0.4  $\mu$ M OREGON-GREEN Taxol bis-acetate OG-taxol (Invitrogen), 0.5  $\mu$ M Calcein-AM (ThermoFisher Sci) or 0.8  $\mu$ M BODIPY-verapamil (Invitrogen). The cells were incubated at 37°C for 20 min before pelleting and washing as before. The cells were then resuspended in 400  $\mu$ l transport buffer and kept on ice until flow cytometry. Single fluorophore samples were also included to control for spectral spillover during flow cytometry. Two-colour flow cytometry was performed on a LSRII (Becton Dickinson). Fluorescence data from 10,000 cells of normal size and granularity were acquired in CellQuest software (Becton Dickinson) and analysed in Flowjo (Becton Dickinson).

#### 2.4 Stable expression of ABCB1 in HEK293 Flp-In cells

HEK293 Flp-In cells with stable expression of ABCB1 wild-type were generated previously (9). The cDNAs encoding ABCB1-Q347/990A and ABCB1-Q347/725/990A were excised from their parent pCI-neo plasmids using *Bam*HI/*Not*I restriction endonuclease double digests and subcloned into the equivalent sites of pcDNA5/FRT (ThermoFisher Sci). The resulting pcDNA5/FRT-ABCB1-Q347/990A and pcDNA5/FRT-ABCB1-Q347/725/990A (Qtriple) were used to co-transfect HEK293 Flp-In cells (ThermoFisher Sci) along with the pOG44 (ThermoFisher Sci) as a source of Flp recombinase as described by the manufacturer. Stable transfected cells (Flp-In ABCB1-Q347/990A, Flp-In ABCB1-Q347/725/990A (Qtriple) and pcDNA/FRT as a vector-only negative control) were selected with hygromycin (200  $\mu$ g/ml) and, once uniform expression of the mutant ABCB1 were confirmed, maintained in hygromycin (100  $\mu$ g/ml).

#### 2.5 Taxol survival curve

Flp-In-ABCB1, Flp-In-ABCB1-Q347/990A, Flp-In ABCB1-Qtriple and Flp-In-vector control cells ( $1 \times 10^4$ ) were seeded into a 96 well dish in 100  $\mu$ l of DMEM with high glucose and 10% FBS but without hygromycin and allowed to attach for several hours. Taxol (Cambridge Bioscience) was added to a final concentration ranging from 0 nM to 10  $\mu$ M and the cells cultured at 37°C in a humidified incubator with 5% CO<sub>2</sub>. After 72 hrs the media was aspirated, the cells were detached with 30  $\mu$ l TrypLE Express (ThermoFisher) which was quenched with 75  $\mu$ l transport buffer and transferred to flow cytometry tubes. The entire population of cells of normal size and granularity, gated on the zero drug condition, were counted in an ACEA NovoCyte flow cytometer (Agilent). Cell number data was analysed in Graphpad Prism version 8. Curve fitting used non-linear regression

### 3. Results

To test the importance of the hydrogen bond donors implicated in the coordination of taxol we effectively removed the donor side chains by site directed mutagenesis and measured the function of the mutant protein in its native environment of live human cells. Function analysis used a modified flow cytometric transport assay to correlate ABCB1 expression with the reduced cellular accumulation of a fluorescent transport substrate normalizing to the untransfected cells in the population.

#### 3.1. Endpoint two-colour flow cytometry assay measures the function of ABCB1 in live cells

HEK293T cells were transfected transiently with pABCB1 encoding wild-type ABCB1. The density of ABCB1 on the cell surface was determined using saturating amounts of the anti-ABCB1 monoclonal antibody (4E3) that does not inhibit transporter function. The primary antibody was detected using saturating amounts of anti-mouse secondary antibody conjugated to a red fluorescent fluorophore. The red fluorescent cells are easily detected by flow cytometry and when they express the wild-type transporter these cells accumulate low levels of green-fluorescent transport substrates or drugs (Figure 1). Transient transfection under the conditions used never results in 100% transfection

efficiency, so there are always non-expressing cells in the population and these become important internal controls. The drug content (green fluorescence) within the ABCB1-negative (untransfected) cells divided by the drug content of the ABCB1-positive cells (equation in Figure 1b) provides a robust and reproducible measure of the functionality of the transporter. The example given in Figure 1 shows a ratio of 96 for Calcein-AM added to a final concentration of 0.5  $\mu$ M.

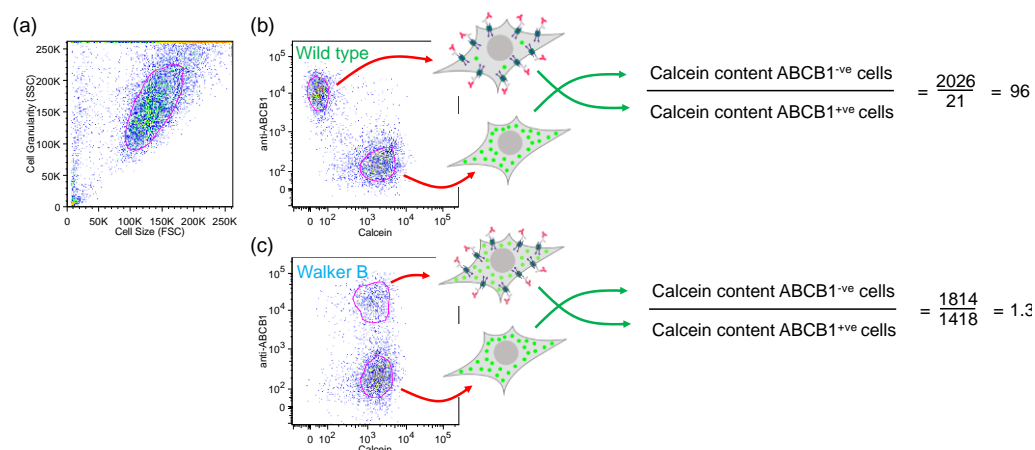


**Figure 1.** Measurement of functionality of ABCB1 for the transport of Calcein-AM by flow cytometry: (a) dotplot showing the gating (autogated population circled in red) of HEK293T cells of normal size and granularity; (b) two-colour dotplot of the gated normal cells showing green-fluorescent Calcein on the x-axis and red-fluorescent antibody binding on the y-axis. Cells that express wild-type ABCB1 bind the anti-ABCB1 antibody (red antibody shapes in the cartoon cell) and have a low level of accumulation of Calcein-AM (green circles in the cartoon cell) whilst untransfected cells accumulate high levels. The ratio of drug accumulation between the ABCB1-expressing and non-expressing cells is used to quantify transporter functionality. (c) Cells expressing the non-functional Walker B mutant (E556/1201Q) accumulate the same level of Calcein-AM as the untransfected cells in the population.

For these data to reflect the functionality of the expressed transporter in a reproducible manner it is important to control two factors. First, the cells must be exposed to a sufficient concentration of drug such that all ABCB1 molecules are required to function to limit drug accumulation. This was determined empirically by exposing the cells to increasing levels of drug to determine the concentration at which the ABCB1-positive cells began to accumulate the green fluorophore. The titration of Calcein-AM is shown in Supplementary Figure S1a and shows that 0.5  $\mu$ M is appropriate. Supplementary figures S1b and S1c show the drug accumulation curves for drugs BODIPY-verapamil and OREGON GREEN taxol bisacetate (OG-taxol), respectively. Second, the experimental set up allows gating on populations of cells that express equivalent levels of the transporter (that have bound equivalent levels of the red fluorescent secondary antibody) as shown for the exemplar Calcein-AM transport experiment in Supplementary Figure S2. This ensures that any differences in drug accumulation between mutants are due to the functionality of the transporter rather than density of the transporters in the plasma membrane.

### 3.2. Q347, Q725 and Q990 modulate the transport of the xanthene dye Calcein-AM

In order to test the importance of the hydrogen bonds formed between taxol and the side chains of ABCB1 amino acids Q347, Q725 and Q990, the wild-type glutamines were replaced with alanine by site-directed mutagenesis. Alanine with its non-polar side chain is unable to donate an equivalent hydrogen bond to the transport substrate but its smaller

side chain should be tolerated in the tertiary structure of the protein. Individual, pairwise and a triple (Qtriple) mutant were generated.

### 3.2.1. Of the single mutants, only Q347A shows a statistically significant reduction in Calcein-AM transport

Single mutants had only a modest effect on the transport of Calcein-AM as shown in the first four columns of Figure 2. Of the single mutants, only Q347A reduced the function of the transporter (to 63% of the wild-type level). Q725A showed a trend towards being more functional than the wild-type but this did not reach statistical significance and no effect was recorded for Q990A. This suggested that none of the hydrogen bonds that can be formed with the side chains of these three glutamines are essential for triggering the transport cycle although it is more efficient at effluxing Calcein-AM with glutamine 347 present.

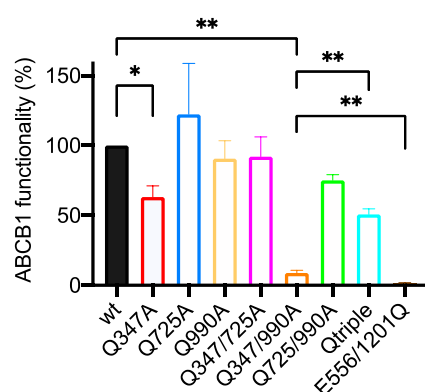


**Figure 2.** Functionality of glutamine to alanine mutants for the transport of Calcein-AM. Live HEK293T cells transiently expressing equivalent amounts of wild-type (wt) and mutant ABCB1 were challenged with Calcein-AM. Functionality was measured as the ratio of Calcein accumulation (Calcein-AM only becomes fluorescent once it is de-esterified) between the ABCB1-expressing and untransfected cells within the population. This was normalised to 100% for wild-type ABCB1 for the bar graph shown. The mean  $\pm$  SEM was plotted using Graphpad Prism version 8; sample number was  $\geq 3$ . Selected statistical analysis (ratio of paired Student's t-test, two-tailed) performed on the raw data is shown with P values: \* $<0.05$ , \*\* $<0.01$ . The full pairwise comparison of the data is given in Appendix Table A1.

### 3.2.2 Q347A and Q990A act synergistically to reduce the transport of Calcein-AM

All three double mutant combinations and the triple mutant (Qtriple) were generated. Their ability to transport Calcein-AM showed pronounced and unexpected differences. A simple additive effect of Q347A and Q990A would predict a functionality of the Q347/990A double mutant to be 57% (the level of functionality of the Q990A mutant multiplied by the level of functionality of the Q347A mutant;  $90/100 \times 63/100 = 57/100$ ). The observed activity of the Q347/990A mutant was reduced to 8.8% of the wild-type transporter suggesting a synergistic effect of the combined mutations and the importance of these two hydrogen bond donors for the efficient efflux of Calcein-AM. However, it is clearly not essential that these two glutamines are present because the 8.8  $\pm$  1.87% (mean  $\pm$  SEM) level of activity remains statistically higher than the Walker B mutant E556/1201Q (1.3  $\pm$  0.59%) which is unable to hydrolyse ATP indicating that the Q347/990A mutant retains measurable function.

### 3.2.3 The Q725A mutation improves the efficiency of transport of Calcein-AM

The most surprising result is that the mutation of glutamine 725 to alanine improves the functionality of ABCB1 for the transport of Calcein-AM. This is most clearly evident when the Q725A mutation is introduced into the Q347/990A background to generate the Qtriple mutant. The Qtriple mutant has a transport activity of 50.7 +/- 4.0% while the Q347/990A double mutant has a transport activity of 8.8 +/-1.9%. The P value for this comparison by Student's t-test is 0.0055, strongly suggesting that the inclusion of the Q725A mutation has made the Qtriple mutant more active than the Q347/990A double mutant and at the same time emphasising that neither Q347 nor Q990 are absolutely necessary for ABCB1 to transport Calcein-AM. The ostensible increase in the mean activities of the other three constructs that include the Q725A mutation when compared to their respective backbones (wild-type versus Q725A, Q347A versus Q347/725A and Q990A versus Q725/990A) fail to reach statistical significance (Table A1).

### 3.3. Q347, Q725 and Q990 also modulate the transport of the phenylalkylamine BODIPY-verapamil

To test whether Q347, Q725 and Q990 are also important for the transport of a different drug class, the transport assays were repeated with a fluorescent derivative of the phenylalkylamine verapamil, which acts as a calcium channel blocker and is used clinically to treat a variety of heart arrhythmias.

#### 3.3.1. Q725A improves the transport activity of BODIPY-verapamil in any background

Challenge with BODIPY-verapamil gave a clearer indication that the side chain of the native Q725 inhibits transport activity (Figure 3). Comparing the raw transport data of the Q725A single mutant with the wild-type transporter, it is statistically clear that Q725A increased the ability to efflux BODIPY-verapamil. This relationship is maintained for all mutants that include Q725A compared to the backbone into which the mutation was introduced. Thus, Q347/725A is statistically more active for the transport of BODIPY-verapamil compared to Q347A, likewise Q725/990A is more active than Q990A, and the Qtriple mutant is more active than Q347/Q990A.

#### 3.3.2. Q347A and Q990A also act synergistically to reduce the transport of BODIPY-verapamil

The Q347A and Q990A mutants (normalized transport activity of 81 +/-8% and 105 +/-16%, respectively (Appendix Table 2)) combine in the Q347/990A double mutant to reduce the transport of BODIPY-verapamil to 38 +/-10% of the wild-type level (Figure 3). This double mutant also retains the ability to efflux BODIPY-verapamil because it is significantly different to the Walker B mutant E556/1201Q.

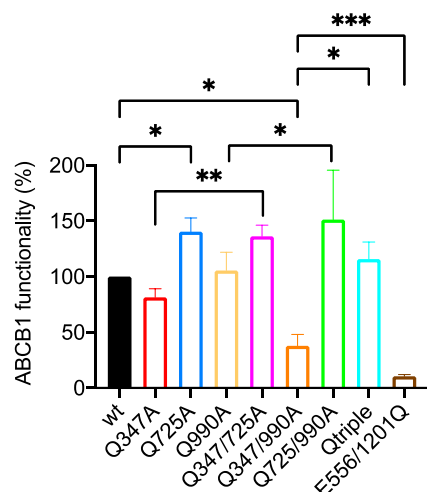


**Figure 3.** Functionality of glutamine to alanine mutants for the transport of BODIPY-verapamil. Live HEK293T cells transiently expressing equivalent amounts of wild-type (wt) and mutant ABCB1 were challenged with BODIPY-verapamil. Functionality was measured as the ratio of BODIPY-verapamil accumulation between the ABCB1-expressing and untransfected cells within the population. This was normalised to 100% for wild-type ABCB1 for the bar graph shown. The mean  $\pm$  SEM was plotted using Graphpad Prism version 8; sample number was  $\geq 3$ . Selected statistical analysis (ratio of paired Student's T-test, two-tailed) performed on the raw data is shown with P values: \* $<0.05$ , \*\* $<0.01$ . The full pairwise comparison of the data is given in Appendix Table A2.

#### 3.4. Q347, Q725 and Q990 have a more limited effect on the transport of the taxane diterpenoid derivative OG-taxol

Taxol, the transport substrate that was first observed in complex with ABCB1 is not fluorescent but its derivative OREGON-GREEN taxol bisacetate (OG-taxol) fluoresces in the green spectrum and retains ability to bind to microtubules in live cells. We tested whether, like taxol itself, it is also a transport substrate of ABCB1. A drug titration experiment showed that ABCB1-expressing cells accumulate less OG-taxol than non-expressing control cells and indicated that 0.4  $\mu$ M OG-taxol was sufficient to require all of the ABCB1 molecules on the surface of our transiently-transfected HEK293T cells to limit accumulation of the drug (Supplementary Figure S1c).

##### 3.4.1. Of the single mutants only Q990A appears to reduce the transport of OG-taxol

The Q347A and Q725A mutants were not distinguishable from the wild-type transport activity. However, the reduced activity of the Q990A mutant reaches statistical significance but only after the raw data are paired (Figure 4). The effect is subtle with the Q990A mutant retaining 66  $\pm$  8 % transport activity for OG-taxol when normalised to wild-type ABCB1.

##### 3.4.2. The double mutants Q347/990A and Q725/990A reduce the transport activity further but the triple mutant restores wild-type levels of OG-taxol transport

The Q347/725A double mutant is trending towards reduced transport of OG-taxol but does not reach statistical significance. However, both Q347/990A and Q725/990A have reduced transport activity for OG-taxol emphasising the negative effect of the Q990A mutation. Perhaps surprisingly, given that all pairwise mutants seem to have reduced transport of OG-taxol, the triple mutant restores transport activity to wild-type levels.

##### 3.4.3 There is no indication that glutamine 725 is inhibitory for the transport of OG-taxol

In contrast to the transport of Calcein-AM and BODIPY-verapamil, there is no evidence from the data that transport of OG-taxol is improved in any mutant harbouring the Q725A change. Although the Q347/990A mutant has a lower mean transport activity (48 +/-9%) than the Qtriple (82 +/-13%) these are not statistically different and none of the other mutants to which Q725A has been introduced come close to a statistically relevant difference to the parent plasmid (e.g. Q990A compared to Q725/990A).

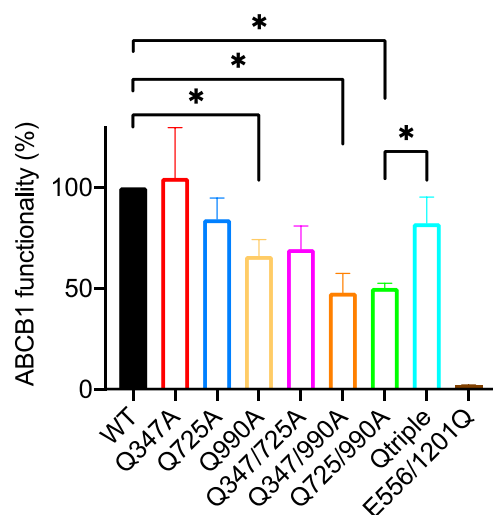


**Figure 4.** Functionality of glutamine to alanine mutants for the transport of OG-taxol. Live HEK293T cells transiently expressing equivalent amounts of wild-type (wt) and mutant ABCB1 were challenged with OG-taxol. Functionality was measured as the ratio of OG-taxol accumulation between the ABCB1-expressing and untransfected cells within the population. This was normalised to 100% for wild-type ABCB1 for the bar graph shown. The mean +/- SEM was plotted using Graphpad Prism version 8; sample number was  $\geq 3$ . Selected statistical analysis (unpaired Student's T-test, two-tailed performed on the raw data except for the comparison of the wild-type with Q990A for which the raw data are paired) is shown with P value: \* $<0.05$ . The full pairwise comparison of the data is given in Appendix Table A3.

### 3.5. The Q347/990A and the Qtriple mutant are indistinguishable from the wild-type transporter in conferring taxol resistance to cells in culture

The more subtle differences observed for the transport of OG-taxol suggested that either the hydrogen bonds donated by Q347, Q725 and Q990 were not particularly important for the transport cycle or that OG-taxol, despite being a transport substrate for ABCB1, does not replicate the geometry of taxol in the binding pocket. To test this, stable cell lines were derived to express the Q347/990A double mutant and the Qtriple mutant. The Q347/990A mutant was chosen because it consistently had the biggest effect on the transport of the three transport substrates tested and the Qtriple was chosen in case the three hydrogen bonds were critical only for the binding of taxol that they had been observed to coordinate. To ensure that like for like comparisons could be made, the cDNAs for Q347/990A and Qtriple were subcloned into pcDNA5/FRT. This allowed site-directed recombination to introduce a single copy of the plasmid into the same site within the genome of Flp-In HEK293. Along with Flp-In-ABCB1wt which was generated previously these stable cell lines ensured uniform levels of wild-type and mutant ABCB1 expression compared with the vector-only (integrated pcDNA5/FRT) negative control (Figure 5a).

The cells lines were challenged with increasing concentrations of taxol for three days, after which the cells with normal size and granularity were counted (Figure 5b; the use of a NovoCyte flow cytometer allowed all cells in the well to be counted in this



experiment thus there is no estimation by counting only a small fraction of population). This allowed the IC<sub>50</sub> for taxol to be calculated for the two test cell lines and compared to positive (cells expressing the wild-type transporter) and negative (cells with an integrated empty vector) controls (Figure 5c). It was clear from the survival curves that taxol is a potent cytotoxic, killing the vector-only control cells with an IC<sub>50</sub> = 5.8 nM. Stable expression of wild-type ABCB1 shifts that IC<sub>50</sub> more than 40-fold to an IC<sub>50</sub> = 240 nM. The measured half maximal inhibitory concentrations for the Flp-In-Q347/990A and Flp-In-Qtriple cells are 430 nM and 480 nM, respectively and are statistically indistinguishable from the effect of taxol on the Flp-In-ABCB1 wild-type cells.

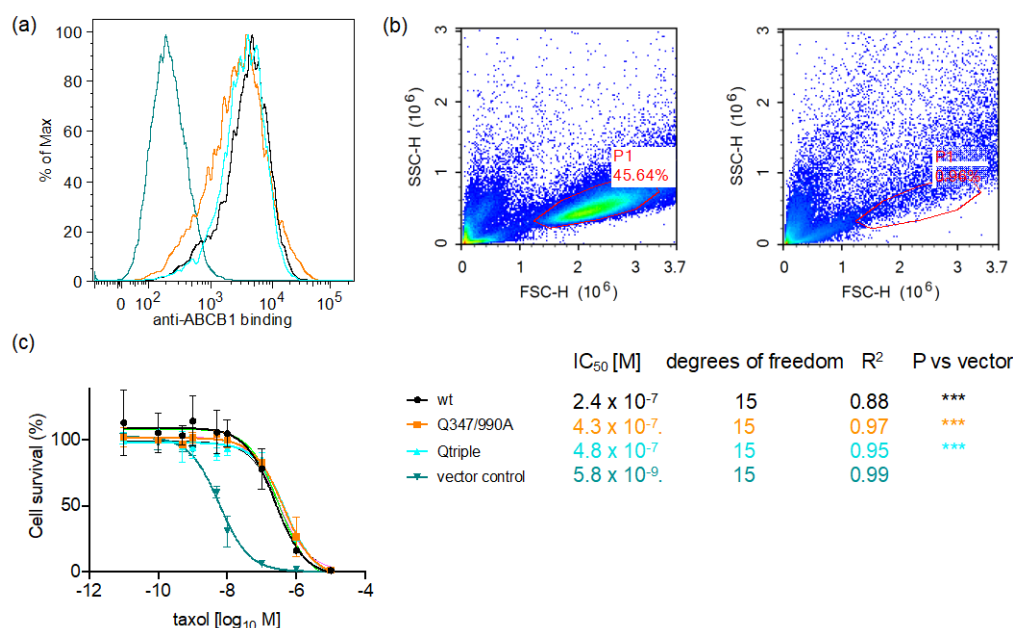


**Figure 5.** Stable expression of ABCB1-Q347/990A or ABCB1-Qtriple confers the same level of resistance to taxol as wild-type ABCB1; (a) Surface expression of ABCB1 (4E3 antibody binding) is similarly elevated for the two mutants (Q347/990A in orange and Qtriple in cyan) and the wild-type transporter (black) compared to the vector-only control (teal); (b) Flow cytometric exemplar dotplots in the presence and absence of taxol. Plots for the Flp-In ABCB1-Q347/990A cell line shows the forward scatter (FSC) and side scatter (SSC) heights in the absence (left hand plot) and the presence of 10 μg/ml taxol for 72 hrs (right hand plot). All cells of normal size and granularity in the well were counted in a NovoCyte flow cytometer and analysed in NovoExoress software. The P1 gate which defines the healthy cell population in the absence of taxol was copied to all other conditions. In the examples shown, there were 71,969 cells in the P1 gate in the absence of taxol and 943 cells in the P1 gate following exposure to 10 μg/ml taxol; (c) Non linear regression analysis of cell survival on challenge with increasing concentration of taxol (colour code as above). Cell number in each well of the taxol dilution series was normalised to 100% for the P1 gate of the zero taxol condition. The mean +/- SEM was plotted with curve fitting by non linear regression in Graphpad Prism version 8; sample number, n = 2 biological repeats. The biological repeats were averaged from duplicate technical repeats. \*\*\* P < 0.0001 compared to the vector-only cell line. The cell lines expressing the double and triple mutant ABCB1 are not significantly different to that expressing the wild-type transporter.

#### 4. Discussion

Structure-activity relationship (SAR) analyses (7), determination of the ABCB1 structure in complex with taxol (6) and molecular modelling studies (10) all implicate the importance of hydrogen bonding between the transporter and the substrates that it transports. Alam *et al.*, (6) highlighted three hydrogen bonds donated by Q347, Q725 and Q990 to coordinate taxol in the binding pocket of ABCB1. We have tested whether this H-bonding pattern was key to triggering the transport cycle with three different

pharmacophores, a xanthene, a phenylalkylamine, and two forms of a taxane diterpenoid. Several conclusions can be drawn from this study with the simplest being that none of these hydrogen bonds are absolutely essential for transport. Even the most impaired double mutant, Q347/990A which has only 8.8 % of the wild-type level of activity for the transport of Calcein-AM, can significantly reduce the accumulation of the dye by cells. For Calcein-AM this equates to an average 25-fold reduction in uptake of the dye compared to untransfected cells which is significantly different to the non-functional Walker B mutant and thus it is clear that these mutant transporters retain transport activity for all three of the different classes of drug tested.

The situation, of course, is more nuanced. There is some consistency in the transport of different drugs, for example, the Q347/990A mutant has significantly reduced activity for the transport of all three fluorescent drugs but the level of impairment is to a different degree (8.8 % of the transport activity of the wild-type for Calcein-AM, 37.8 % for BODIPY-verapamil and 48 % for OG-taxol). Thus it would appear that the hydrogen bonding capacity of the side chains of Q347 and Q990 are involved in drug transport. There are also drug specific effects; there is a clear indication that introduction of the Q725A mutation improves the transport of Calcein-AM (cf. Q347/990A and Qtriple) and BODIPY-verapamil but this is not true for OG-taxol. Perhaps the most surprising finding was that the Qtriple mutant, in which all three glutamines are placed by alanine, retained activity (or regained activity compared to some double mutants) for the transport of all three drugs to achieve 51 % transport activity for Calcein-AM, 116 % activity for BODIPY-verapamil and 82 % activity for OG-taxol. This observation also emphasizes that Q347 and Q990 are not critical for the efficient transport because they are also absent from the Qtriple mutant which is indistinguishable from the wild-type transporter for the transport of BODIPY-verapamil and OG-taxol. This negative effect of Q725 on transport activities that we observe is consistent with an earlier study by Loo *et al.*, (11) during which they characterized a Q725C mutant (in an otherwise cysteine-less version of ABCB1). They observed that the basal ATPase activity of Q725C measured *in vitro* was raised 2.6-fold offering a possible explanation for the improved transport of BODIPY-verapamil and Calcein-AM by Q725A mutants that may be unrelated to the binding affinity of the drugs.

The prevention of fluorescent drug accumulation is a robust test of the ABCB1 transport cycle and it has the advantage of measuring ABCB1 function in live cells in its native environment of the plasma membrane. However, the flow cytometric assay does have the limitation of being dependent on fluorescent dyes and drug analogues. In OG-taxol, while the oxygen atoms in the taxol pharmacophore that were observed to hydrogen bond with Q347, Q725 and Q990 remain available, the molecular weight of the fluorescent drug is 1.5 times greater than that of the taxol which must affect the geometry of the interaction of the drug within the binding pocket. To rule out a possible artefact we generated stable cell lines and demonstrated that the mutant transporters Q347/990A and the Qtriple conferred resistance to taxol to the same degree as the wild-type transporter. So, in a direct test against unmodified taxol that would be unable to hydrogen bond with the side chains of alanines at positions 347 and 990 (plus or minus position 725) we observed no difference in the survival curves of ABCB1-expressing cells, making it clear that the hydrogen bonds observed in the cryoEM data are not particularly important for the function of the transporter.

A second structure of ABCB1 in complex with a transport substrate, the vinca alkaloid vincristine, has now been reported by Nosol *et al.*, (12). The binding pocket of vincristine overlaps with that of taxol sharing six amino acids in common, including Q347 and Q990 (the latter considered close enough to hydrogen bond). Six further amino acids are unique to the vincristine pocket and five more for taxol; some of these differences involve a subtle turn of a helix (for example Y307 in TMH5 is implicated in taxol binding while the adjacent amino acid I306 is implicated in vincristine binding). The main

contributors to both binding pockets are from TMH5, 6, 11 and 12 while the vincristine pocket also includes M68 and M69 from TMH1 and E875 from TMH10, and the taxol pocket includes Q725 from TMH7. It is perhaps not coincidental that Seelig had already noted in 1998 that TMH4, 5, 6, 11 and 12 are enriched in amino acids with hydrogen bond donor side chains (7). So, is it possible to reconcile the drug SAR data, the empirical structural data, and the mutagenesis and drug transport contained herein if the transmembrane domains are sufficiently flexible to fold around the transport substrate? An induced fit model has long been postulated to explain the unusually broad polyspecificity of ABCB1 and the first evidence in support of induced fit was reported by Clarke's group in 2003 in which they showed a changing cross-linking pattern within the transmembrane domains in response to different drugs (13). With this in mind, it seems perfectly reasonable to suggest that taxol might hydrogen bond to Q347, Q725 and Q990, but in their absence, different hydrogen bonds (or other electrostatic or weaker Van der Waals interactions) may be formed as the transmembrane domains close around the drug in the cavity. Further experiments will be required to test whether the lack of effect of the double or triple alanine mutants are due to redundancy among the hydrogen bond donors within ABCB1 but, for sure, neither Q347, Q725 nor Q990 are essential for taxol efflux.

**Supplementary Materials:** The following are available online at [www.mdpi.com/xxx/s1](http://www.mdpi.com/xxx/s1), Figure S1: Titration of transport substrates for development of flow cytometry assay. Figure S2: Confirmation of equivalent levels of ABCB1 at the plasma membrane ensured that any differences in transport activity were due to ABCB1 functionality rather than the transporter expression level.

**Author Contributions:** Conceptualization, K.J.L.; formal analysis, K.J.L and F.B.; investigation, K.S., H.A.I., A.O. and K.J.L.; data curation, K.J.L.; writing—original draft preparation, K.J.L.; writing—review and editing, K.S., H.A.I., A.O., F.B. and K.J.L.; supervision, K.J.L. All authors have read and agreed to the published version of the manuscript.

**Funding:** This research received no external funding.

**Data Availability Statement:** The raw data and materials generated in this study are available directly from K.J.L.

**Acknowledgments:** The authors would like to thank Dr Gary Warnes, manager of the flow cytometry facility in the Blizzard Institute for guidance and help with the flow cytometers and flow cytometry software used in this study.

**Conflicts of Interest:** The authors declare no conflict of interest.

## Appendix A

**Table A1.** Functionality of mutants for the transport of Calcein-AM normalised to the wild-type transporter and pairwise statistical comparison of the raw data.

	Wild type 100%	E556/1201Q 1.3 ±0.6	Q347A 63.1 ±8.0	Q725A 122.3 ±36.4	Q990A 90.7 ±12.8	Q347/725A 92.1 ±14.2	Q347/990A 8.8 ±1.8	Q725/990A 75.1±4.0
E556/1201Q 1.3 ±0.6	<0.0001 ****	-						
Q347A 63.1 ±8.0	0.0363 *	0.0061 **	-					
Q725A 122.3 ±36.4	ns	0.0379 *	ns	-				
Q990A 90.7 ±12.8	ns	0.0025 **	0.0485 *	ns	-			
Q347/725A 92.1 ±14.2	ns	0.0002 ***	ns	ns	ns	-		
Q347/990A 8.8 ±1.8	0.0097 **	0.0024 **	0.0025 **	0.0358 *	0.0031 **	0.0010 **	-	
Q725/990A 75.1 ±4.0	0.0301 *	0.0005 ***	ns	ns	ns	ns	0.0106 *	-
Qtriple 50.7 ±4.0	0.0131 *	0.0031 **	ns	ns	ns	0.0296 *	0.0055 **	ns

The raw data has been used for statistical comparisons. Ratio, paired Student's t-test was used for all comparisons to wild-type ABCB1 and the Walker B mutants E556/1201A activities because these positive and negative controls were included in every experiment. Where this was not possible (because of the large the number of mutants tested and when their construction was completed), unpaired Student's t-test was applied to the data normalized to one hundred percent wild-type activity (highlighted in yellow).

**Table A2.** Functionality of mutants for the transport of BODIPY-verapamil normalised to the wild-type transporter activity and pairwise statistical comparison of the raw data.

	Wild type 100%	E556/1201Q 10.5 ±1.6	Q347A 81.4 ±7.7	Q725A 140.5 ±12.3	Q990A 105.6 ±16.3	Q347/725A 136.3 ± 10.0	Q347/990A 37.9 ±10.1	Q725/990A 151.3 ±44.3
E556/1201Q 10.5 ±1.6	<0.0001 ****	-						
Q347A 81.4 ±7.7	ns	0.0007 ***	-					
Q725A 140.5 ±12.3	0.0410 *	<0.0001 ****	0.0061 **	-				
Q990A 105.6 ±16.3	ns	0.0026 **	ns	ns	-			
Q347/725A 136.3 ± 10.0	ns	0.0040 **	0.0089 **	ns	0.0422 *	-		
Q347/990A 37.9 ±10.1	0.0258 *	0.0042 **	ns	0.0029 **	ns	ns	-	
Q725/990A 151.3 ±44.3	ns	0.0032 **	0.0018 **	0.0286 *	0.0182 *	ns	0.0225 *	-
Qtriple 115.7 ±15.3	ns	0.0008 ***	0.0022 **	ns	ns	ns	0.0300 *	ns

The raw data has been used for statistical comparisons. Ratio, paired Student's t-test was used for all comparisons to wild-type ABCB1 and the Walker B mutants E556/1201A as above. Where this was not possible unpaired Student's t-test was applied to the raw data (highlighted in yellow).

**Table A3.** Functionality of mutants for the transport of OREGON-GREEN taxol bisacetate normalised to the wild-type transporter activity and pairwise statistical comparison of the raw data.

	Wild type 100 %	E556/1201Q 2.0 ±0.2	Q347A 104 ±25	Q725A 84 ±10	Q990A 66 ±8	Q347/725A 69 ±11	Q347/990A 48 ±9	Q725/990A 50 ±2
E556/1201Q 2.0 ±0.2	0.0075 **	-						
Q347A 104 ±25	ns	0.0148 *	-					
Q725A 84 ±10	ns	0.0032 **	ns	-				
Q990A 66 ±8	0.0467 *	0.0034 **	ns	ns	-			
Q347/725A 69 ±11	ns	0.0003 ***	ns	ns	ns	-		
Q347/990A 48 ±9	0.0184 *	0.0001 ***	ns	ns	ns	0.0292 *	-	
Q725/990A 50 ±2	0.0290 *	0.028 *	0.0203 *	0.0305 *	ns	0.0234 *	ns	-
Qtriple 82 ±13	ns	0.0231 *	ns	ns	ns	ns	ns	0.027 *

Unpaired Student's t-test on the raw data was used for all comparisons except for Q990A vs wild-type where a paired Student's t-test was applied to the raw data (highlighted in yellow).

## References

1. Robey RW, Pluchino KM, Hall MD, Fojo AT, Bates SE, Gottesman MM. Revisiting the role of ABC transporters in multidrug-resistant cancer. *Nat Rev Cancer*. 2018;18(7):452-64.
2. Gottesman MM. Mechanisms of cancer drug resistance. *Annu Rev Med*. 2002;53:615-27.
3. Maloney SM, Hoover CA, Morejon-Lasso LV, Prospero JR. Mechanisms of Taxane Resistance. *Cancers (Basel)*. 2020;12(11).
4. Gottesman MM, Pastan IH. The Role of Multidrug Resistance Efflux Pumps in Cancer: Revisiting a JNCI Publication Exploring Expression of the MDR1 (P-glycoprotein) Gene. *J Natl Cancer Inst*. 2015;107(9).
5. Nigam SK. What do drug transporters really do? *Nat Rev Drug Discov*. 2015;14(1):29-44.
6. Alam A, Kowal J, Broude E, Roninson I, Locher KP. Structural insight into substrate and inhibitor discrimination by human P-glycoprotein. *Science*. 2019;363(6428):753-6.
7. Seelig A. A general pattern for substrate recognition by P-glycoprotein. *Eur J Biochem*. 1998;251(1-2):252-61.
8. Seelig A, Landwojtowicz E. Structure-activity relationship of P-glycoprotein substrates and modifiers. *Eur J Pharm Sci*. 2000;12(1):31-40.
9. Akkaya BG, Zolnerciks JK, Ritchie TK, Bauer B, Hartz AM, Sullivan JA, et al. The multidrug resistance pump ABCB1 is a substrate for the ubiquitin ligase NEDD4-1. *Molecular membrane biology*. 2015;32(2):39-45.
10. Mora Lagares L, Minovski N, Novic M. Multiclass Classifier for P-Glycoprotein Substrates, Inhibitors, and Non-Active Compounds. *Molecules*. 2019;24(10).
11. Loo TW, Bartlett MC, Clarke DM. Transmembrane segment 7 of human P-glycoprotein forms part of the drug-binding pocket. *Biochem J*. 2006;399(2):351-9.
12. Nosol K, Romane K, Irobalieva RN, Alam A, Kowal J, Fujita N, et al. Cryo-EM structures reveal distinct mechanisms of inhibition of the human multidrug transporter ABCB1. *Proc Natl Acad Sci U S A*. 2020;117(42):26245-53.
13. Loo TW, Bartlett MC, Clarke DM. Substrate-induced conformational changes in the transmembrane segments of human P-glycoprotein. Direct evidence for the substrate-induced fit mechanism for drug binding. *J Biol Chem*. 2003;278(16):13603-6.